Combined spectroscopic study on the growth mechanism of Diphosphine-stabilized Gold Nanoclusters

Jie Bao, Lina Yang, Wei Liu, Yuanyuan Huang, Ting Huang, Yuanjie Cao, Tao Yao*, Zhihu Sun*, and Shiqiang Wei

National Synchrotron Radiation Laboratory, University of Science and Technology of China, Hefei 230029, P.R. China.

∗Corresponding author. E-mail: yaot@ustc.edu.cn , zhsun@ustc.edu.cn

ABSTRACT: The formation process of 1,5-Bis(diphenylphosphino) pentane (L^5)-protected Au nanocluster through the reduction of precursor $Au_2L^5Cl_2$ by borane-tert-butylamine (TBAB) is traced by a combination of time-dependent x-ray/UV-vis absorption spectroscopies and mass spectrometry. It is revealed that the initial generation of dual-core basic unit $Au_4L^5_2Cl$ is a critical step, which allows for a subsequent size-growth process via incorporation of the existing Au monomer (Au(I)-Cl) or Au_2L^5 to form $Au_5L^5_2$, $Au_8L^5_3Cl$, $Au_{10}L^5_4Cl$ and finally main $Au_{11}L^5_4Cl_2$. This work advances one step further toward understanding the mechanism of formation and growth of diphosphine ligands-protected Au NCs.

1. Introduction

Small metal clusters composed of a few to tens of core atoms have size-specific unusual physical and chemical properties that differ from those of larger nanocrystals, which have potential applications in fields such as catalysis, optical devices and imaging [1-3]. Particularly, major advances in the chemical solution synthesis of Au nanoclusters has been achieved, and some well-defined thiolate-protected nanoclusters such as Au_{25} and Au_{38} have been reported [4, 5].

Recently, diphosphine ligands have shown promise for facilitating the formation of smaller monodispersed Au clusters [6-8]. Understanding the growth mechanism of the gold-phosphine clusters is necessary for designing synthetic protocols to produce specific nuclearity clusters, and has recently attracted considerable interest [9, 10]. Moreover, it is highly desirable to develop synthetic strategies that permit the precise and efficient synthesis of nanoclusters for fundamental studies as well as practical applications. This requires a profound understanding of the underlying mechanism governing the formation of the nanoclusters.

In this work, we combine the quick X-ray absorption fine structure (XAFS) and UV−vis absorption spectroscopies, as well as matrix-assisted laser desorption ionization mass spectrometry (MALDI-MS) to probe the formation process of the 1,5-bis(diphenylphosphino) pentane (L^5)-protected Au nanocluster.

2. Experimental

Chlorogold(I) diphosphine complexes of $Au_2L^5Cl_2$ were prepared according to the literature for other Au(I)-diphosphine compounds [11]. Then 36.5 mg (0.04 mmol) $Au_2L^5Cl_2$ was disolved in 4 mL ethanol solution, to which an ethanol solution (2 mL) of borane-tert-butylamine (TBAB, 3.5 mg, 0.04 mmol) was quickly added at room temperature under magnetic stirring. At different reaction intervals, aliquotes of the reacting solution were quickly taken from the flask and subjected to characterization. Au L_3-edge XAFS spectra were measured in the quick-XAFS mode (30 sec per scan) at the 1W1B beamline of Beijing Synchrotron Radiation Facility (BSRF), China. The electron storage ring was operated at 2.5 GeV with a maximum current of 250 mA. A double Si (111) crystal monochromator was used. The measurements were performed in the tramsission mode, by using a 10-mm-thick Teflon cell. As a reference, the initial precursor solution prior to TBAB addition was also measured and labeled as 0 min. The UV-vis absorption data were acquired with a Purkinje General TU-9001 spectrometer in the wavelength range of 250–800 nm. Matrix-assisted laser desorption ionization mass-spectrometry (MALDI-MS) measurements were performed with a Bruker Autoflex III mass spectrometer in positive linear mode.

3. Results and discussion

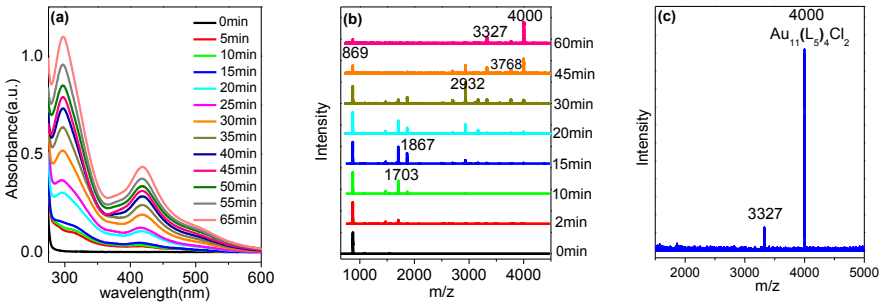

Figure 1. (a) Time-dependent UV-vis absorption spectra and (b) MALDI-MS during the Au cluster formation in ethanol. (c) MALDI-MS of the final product after 24 h of reaction.

Shown in Figure 1(a) are the time-dependent UV-vis absorption spectra. In the initial 15 min, two subtle absorption peaks at about 317 and 420 nm appears, and the first peak broadens. At 20 min, the peak at 317 nm blue shifts to 297 nm, and as the reaction going on, these two peaks at 297 and 420 nm become progressively intensified, while their positions and spectral shape remain unchanged. It is reported that the 420 nm band mainly comprise the contributions from members of the phosphine-ligated Au_x ($8 \le x \le 12$) [9, 12], where the similar charge density transfer between the metal core and the phenyl group and phosphine group result in the similar shape but different intensity [13]. Therefore, the gradually pronounced absorption peaks in the UV-vis spectra, along with the unchanged spectral shape, suggest the growth toward Au_8-Au_{12} clusters after 20 min of reactions. To identify the intermediate species, time-dependent MALDI-MS were measured as displayed in Figure 1(b). In the first 10 min, the formation of $Au_4L^5{}_2Cl$ intermediate cluster is indicated by the peak at m/z=1703 Da, followed by the appearance of another peak at m/z=1867 Da corresponding to $Au_5L^5{}_2$ at 15 min. After that, $Au_4L^5{}_2Cl$ and $Au_5L^5{}_2$ gradually disappeared, and the $Au_7L^5{}_3$ (m/z=2700 Da) and $Au_8L^5{}_3Cl$ (m/z=2932 Da) species emerged simultaneously. At further prolonged reaction times >30 min, end product of Au_{10}-Au_{11} clusters (m/z=3327-4000 Da) with the dominant $Au_{11}L^5{}_4Cl_2$ (m/z =4000 Da) were formed (Fig. 1(c)), which coincides with the UV results.

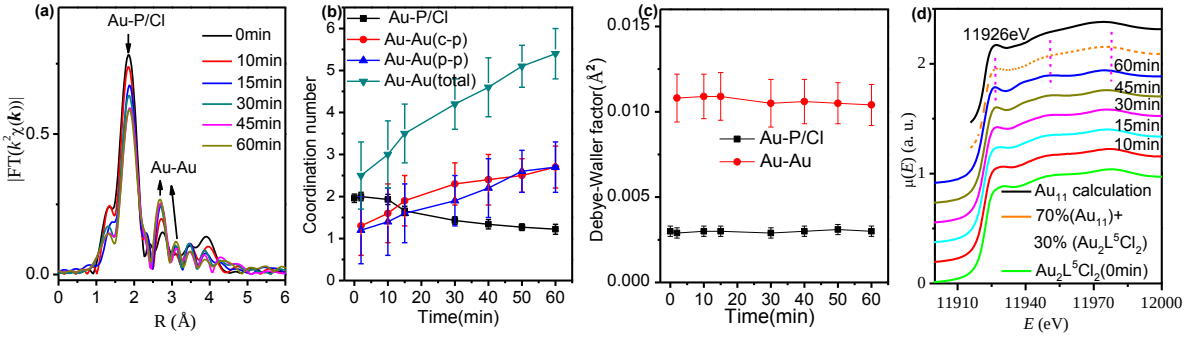

Figure 2. (a) Magnitudes of Foruier-transformed EXAFS $k^2\chi(k)$ functions at typical reaction times. Temporal evolution of coordination number CNs (b), and Debye-Waller factor σ^2 (c) for the Au–P/Cl and Au–Au coordination pairs extracted from EXAFS curve-fitting. (d) XANES spectra at typical reaction times. The calculated XANES spectrum for a $Au_{11}P_8Cl_2$ cluster is also displayed, along with a linear combination of the spectra of $Au_{11}P_8Cl_2$ (70%) and $Au_2L^5Cl_2$ (30%).

To obtain structure and composition information in the reaction process, we performed time-dependent Au L_3-edge XAFS measurements. The EXAFS data processing and curve-fitting were done using the ATHENA and ARTEMIS modules implemented in the IFEFFIT software packages[14], respectively. The quantitative curve-fittings were carried out in the *R*-space with a Fourier transform *k*-space range of 3.0–12.0 $Å^{-1}$. The backscattering amplitudes $F(k)$ and phase-shifts $\Phi(k)$ of the Au−P and Au−Au pairs were calculated for a $Au_{11}P_8Cl_2$ cluster [15, 16] by using FEFF8.0 code [17]. In the incomplete icosahedron of Au_{11}, the central-peripheral and peripheral-peripheral Au−Au bonds are quite different (2.60−2.72 Å *vs* 2.84−3.19 Å)[16], hence two Au−Au pairs labelled as Au−Au (c-p) and Au−Au (p-p) were considered. During the curve-fitting, the overall amplitude reduction factor S_0^2 was fixed to the best-fit value of 0.90 determined from fitting the data of Au foil. For each pair, four parameters of coordination number (CN) *N*, interatomic distance *R*, Debye–Waller factor σ^2, and energy shift ΔE_0 were allowed to vary. To reduce the number of adjustable parameters, a common σ^2 and a common ΔE_0 were used for the two Au-Au pairs.

The magnitudes of the Fourier transformed (FT) EXAFS $k^2\chi(k)$ functions at typical reaction times are shown in Figure 2(a). Evidently, with the increase of reaction time, the Au-ligand (Au−P or Au−Cl, undistinguishable) peak at 1.9 Å is weakened gradually, while the Au-Au peaks (2.7 and 3.1 Å) are significantly intensified, suggesting the gradual growth of the Au clusters. More quantitative results of the cluster growth could be obtained from the least-squares EXAFS curve-fittings. The obtained *N* and σ^2 as functions of reaction time are shown in Figure 2(b) and (c), respectively. At 30 min, the total N_{Au-Au} (4.2) is very close to the nominal N_{Au-Au} (4) of $Au_8L^5{}_3Cl$ [18], and the end product with total N_{Au-Au} of 5.4 is very close to the N_{Au-Au} (5.5) of $Au_{11}L^5{}_4Cl_2$ [15, 16], consistent with the MS results that demonstrate the main products of $Au_8L^5{}_3Cl$ and $Au_{11}L^5{}_4Cl_2$ at 30 and 60 min, respectively. Moreover, at 60 min the Au-ligand CN (1.22) is between the nominal values in the end product of $Au_{11}L^5{}_4Cl_2$ (0.91) and the precursor $Au_2L^5Cl_2$ or analogues (2.0)[15, 16, 19], suggesting the coexistence of both species. The real Au-ligand CN could be roughly expressed as a weighted-sum of the CNs in $Au_{11}L^5{}_4Cl_2$ and $Au_2L^5Cl_2$ *via* $0.91\times p+2\times(1-p)=1.22$, which gives the proportion *p* of Au atoms in $Au_{11}L^5{}_4Cl_2$ as $p\sim0.7$. This point is also supported by the XANES spectra (Fig. 2(d)). The starting material $Au_2L^5Cl_2$ shows a double-peak structure in the white-line region of XANES. With reaction going on, the double-peak disappears and a peak at 11926 eV is gradually intensified. Using the FEFF8.0 code [17], we calculated the spectrum of the $Au_{11}P_8Cl_2$ cluster. A linear combination of the spectrum of $Au_{11}P_8Cl_2$ (70%) and $Au_2L^5Cl_2$ (30%) could well reproduce the main experimental features at 60 min, as labelled by the

vertical bars in Fig. 2(d). These results lead us to conclude that the majority (~70%) of Au atoms are in the form of Au_{11} cluster after 60 min, with a small part (~30%) existing as $Au_2L^5Cl_2$ or other analogous species.

Finally, we discuss briefly the formation mechanism of Au nanoclusters through the reduction of the precursor $Au_2L^5Cl_2$. Yao et al. have reported an initial nucleation of gold nanocrystals by formation of intermediate Cl^{3-}-Au-$AuCl^{3-}$dimer [20]. Analogously, we speculate that two precursor molecules of $Au_2L^5Cl_2$ may form a dual-core basic unit $Au_4L^5_2$ by connecting two Au_2L^5 units, due to the breaking of the Au-Cl bonds under the reduction reaction of TBAB. Then a Au monomer (Au(I)-Cl) which could be formed from $Au_2L^5Cl_2$ by breaking the Au-P bond (and Au-Cl bond) could be linked to the dual-core basic unit to form $Au_5L^5_2$. After that the larger clusters such as $Au_7L^5_3$, $Au_8L^5_3Cl$, $Au_{10}L^5_4Cl$ and $Au_{11}L^5_4Cl_2$ are formed on the basis of the $Au_5L^5_2$, via incorporation of the existing Au monomer (Au(I)-Cl) or Au_2L^5.

4. Conclusions

In summary, using a combination of time-dependent UV-vis/ XAFS and mass spectra, the formation process of L^5-protected Au nanocluster through the reduction of precursor $Au_2L^5Cl_2$ by TBAB is investigated. It is found that the cluster formation is achieved in a nucleating/growth manner including two distinct reaction steps. The initial generation of dual-core basic units of $Au_4L^5_2$ and $Au_5L^5_2$ is a critical step allowing for subsequent size-growth process. This work deepens understanding of the mechanism of formation and growth of diphosphine ligands-protected Au nanoclusters and may be helpful for further controllable synthesis of metal nanoclusters.

Acknowledgments

This work was supported by the National Natural Science Foundation of China (Grant No. 11175184, 11135008, 11475176, 11422547, 11435012, 21471143 and U1332131). The authors are grateful to BSRF for the valuable synchrotron radiation XAFS beamtime.

References

[1] Spivey J J, Krishna K S and Kumar C 2014 *J.Phys.Chem.C* **118** 20043-69
[2] Lu Y Z and Chen W 2012 *Chem.Soc.Rev.* **41** 3594-623
[3] Jin R C 2010 *Nanoscale* **2** 343-62
[4] Qian H F, Zhu Y and Jin R C 2009 *Acs Nano* **3** 3795-803
[5] Wu Z, Suhan J and Jin R C 2009 *J. Mat.Chem.* **19** 622-6
[6] Shichibu Y, Suzuki K and Konishi K 2012 *Nanoscale* **4** 4125-9
[7] Shichibu Y and Konishi K 2010 *Small* **6** 1216-20
[8] Chen J, Zhang Q F and Bonaccorso T 2014 *J.Am.Chem.Soc.* **136** 92-5
[9] Hudgens J W, Pettibone J M and Senftle T P 2011 *Inorg.Chem.* **50** 10178-89
[10] Guidez E B, Hadley A and Aikens C M 2011 *J.Phys.Chem.C* **115** 6305-16
[11] Brandys M C, Jennings M C and Puddephatt R J 2000 *J.Chem.Soc.Dalton* 4601-6
[12] Pettibone J M and Hudgens J W 2010 *J.Phys.Chem.Lett.* **1** 2536-40
[13] Wu Z K and Jin R C 2013 *Chemistry* **19** 12259-63
[14] Newville M 2001 J.Synchrotron Rad. **8** 96-100
[15] McKenzie L C, Zaikova T O and Hutchison J E 2014 *J.Am.Chem.Soc.* **136** 13426-35
[16] Hall K P and Mingos D M P 1984 Prog. Inorg. Chem.**32** 237-325
[17] Ankudinov A L, Ravel B, Rehr J J and Conradson S D 1998 *Phys.Rev.B* **58** 7565-76.
[18] Vandervelden J W A, Bour J J, Bosman W P and Noordik J H 1983 *Inorg.Chem.* **22** 1913-8
[19] Pettibone J M and Hudgens J W 2012 Small **8** 715-25
[20] Yao T, Sun Z H , Li Y Y and Wei S Q 2010 *J.Am.Chem.Soc.* **132** 7696-701